Reprinted from The Journal of Physical Chemistry, 1986, 90, 1436 Copyright © 1986 by the American Chemical Society and reprinted by permission of the copyright owner.

## Mutual Orientation Effects on Electron Transfer between Porphyrins

Robert J. Cave. Paul Siders. and R. A. Marcus\*

Arthur Amos Noyes Laboratory of Chemical Physics, California Institute of Technology, Pasadena. California 91125, and Radiation Laboratory, University of Notre Dame, Notre Dame, Indiana 46556 (Received: August 26, 1985)

Mutual orientation effects on the rate of nonadiabatic electron transfer between several diporphyrin pairs of experimental interest are examined. The electronic matrix element for electron transfer is calculated within a one-electron spheroidal model for a variety of states and orientations which are relevant to both biological and synthetic electron-transfer systems. Both the mutual orientation of the pairs and the nodal structure of the donor and acceptor orbitals can have large effects on calculated rates.

#### I. Introduction

As increasingly detailed information is obtained on the rates and mechanisms of electron-transfer reactions, it has become evident that a more complete understanding is desirable of how the separation distance and mutual orientation of a reactant pair affect the rate. This is especially true for biologial and biomimetic electron-transfer pairs.1

For example, cytochrome c is a widely studied biological electron-transfer agent.<sup>2</sup> The heme is oriented with respect to the protein and has one edge exposed to the solution environment. Its reactions have been discussed in this context.3 Many other biological electron transfers occur between molecules held rigidly at fixed distances and orientations. The electron-transfer rate has been measured for a [ZnII, FeIII] hybrid hemoglobin, for which both the orientation and separation distance of the two porphyrins are known.4 Relative orientations of biological electron-transfer pairs are under study: It has been reported that the molecular planes of the heme c and d groups in cytochrome c-d of Pseudomonas aeruginosa are perpendicular to one another in both the reduced and oxidized forms of the protein.<sup>5</sup> Also, the relative orientations of the initial charge-transfer agents of photosynthetic reaction centers<sup>6</sup> have been determined.

Synthetic systems have also exhibited possible orientation-dependent electron transfers. Photoexcited electron transfer has been observed in the cofacial diporphyrins of Chang,<sup>7</sup> and it has been found to proceed rapidly in the forward direction and considerably slower in the reverse. 8-10 Systems that are similar, but where the transition moments of the two porphyrin subunits are oriented perpendicularly, rather than parallel, have been examined by Overfield et al. 11,12 They show much slower forward transfer than those of ref 7-10.11,12 Separation-distance effects have been examined in rigidly linked porphyrin-quinone systems, 13 so chosen because biological electron transfers frequently involve aromatic donors and acceptors such as porphyrins, porphyrin derivatives, and quinones. In addition, charge-transfer and crystallographic studies have been made of another set of donor-acceptor pairs linked as metacyclophanes and paracyclophanes.14 Also, it has been proposed that electron-transfer fluorescence quenching of chlorophyll a by quinone multilayer arrays requires a favorable orientation of reactants and products.15

Orientation effects have been studied theoretically by using a variety of models<sup>16-22</sup> to examine qualitative effects. Orientation effects have also been examined in studies of the ordering of spin states in compounds containing two metal centers, 23-25 a problem analogous to intramolecular electron transfer.<sup>26</sup> We have recently described a simple model for orientation effects<sup>27</sup> based on the delocalized nature of  $\pi$ -electrons in aromatic systems. It is a one-electron model in which the transferable electron is assumed to be bound at an oblate-spheroidal potential well of specified

depth. Electron transfer was modeled between two such nonpenetrating sites, and the effects of orientation on the thermal matrix element (the electronic matrix element appearing in theories of nonadiabatic electron transfer<sup>28-30</sup>) were examined for various separation distances.

In the present paper the model of ref 27 is applied to a number of systems of experimental interest, both biological and synthetic. The aim of the model is to illustrate possible effects of orbital and

- Boxer, S. G. Biochim. Biophys. Acta 1983, 726, 265-292.
   Dickerson, R. E.; Timkovich, R. In "The Enzymes"; Boyer, P. D., Ed.;
- Academic Press: New York, 1975; Vol. 11, pp 397-547
- (3) Marcus, R. A.; Sutin, N. Biochim. Biophys. Acta 1985, 811, 265-322. (4) McGourty, J. L.; Blough, N. V.; Hoffman, B. M. J. Am. Chem. Soc. 1983, 105, 4470-4472
- (5) Makinen, M. W.; Schichman, S. A.; Hill, S. C.; Gray, H. B. Science 1983, 222, 929-931
- (6) Deisenhofer, J.; Epp, O.; Miki, K.; Huber, R.; Michel, H. J. Mol. Biol. 1984, 180, 385-398.
- (7) Chang, C. K. J. Heterocycl. Chem. 1977, 14, 1285-1288.
  (8) Netzel, T. L.; Kroger, P.; Chang, C.-K.; Fujita, I.; Fajer, J. Chem. Phys. Lett. 1979, 67, 223-228.
- (9) Fujita, I.; Fajer, J.; Chang, C.-K.; Wang, C.-B.; Bergkamp, M. A.; Netzel, T. L. J. Phys. Chem. 1982, 86, 3754-3759.
- (10) Netzel, T. L.; Bergkamp, M. A.; Chang, C.-K. J. Am. Chem. Soc. 1982, 104, 1952–1957.
- (11) Overfield, R. E.; Scherz, A.; Kaufmann, K. J.; Wasielewski, M. R.
- J. Am. Chem. Soc. 1983, 105, 4256–4260.
  (12) Overfield, R. E.; Scherz, A.; Kaufmann, K. J.; Wasielewski, M. R. J. Am. Chem. Soc. 1983, 105, 5747–5752.
- (13) Wasielewski M. R.; Niemczyk, M. P. J. Am. Chem. Soc. 1984, 106,
- 5043-5045 (14) Staab, H. A.; Reibel, W. R. K.; Krieger, C. Chem. Ber. 1985, 118, 1230-1253 and references cited therein. Vogler, H.; Schanne, L.; Staab, H.
- A. Ibid. 1985, 118, 1254-1260.
- (15) Dodelet, J.-P.; Lawrence, M. F.; Ringuet, M.; Leblanc, R. M. Photochem. Photobiol. 1981, 33, 713-720.
  - (16) Ratner, M. A.; Madhukar, A. Chem. Phys. 1978, 30, 201-215.
  - (17) Rice, S A.; Pilling, M. J. Prog. React. Kinet. 1978, 9, 93-194.
    (18) Brocklehurst, B. J. Phys. Chem. 1979, 83, 536-543.
- (19) Doktorov, A. B.; Khairutdinov, R. F.; Zamaraev, K. I. Chem. Phys. 1981, 61, 351-364.
  - (20) Larsson, S. J. Am. Chem. Soc. 1981, 103, 4034-4040.
- (21) Larsson, S. J. Phys. Chem. 1984, 88, 1321-1323.
- (22) Newton, M. D. Int. J. Quantum Chem., Quantum Chem. Symp. 1980, No. 14, 363-391.
- (23) Hay, P. J.; Thibeault, J. C.; Hoffman, R. J. Am. Chem. Soc. 1975, 97, 4884-4899.
- (24) Hodgson, D. J. In "Extended Interactions between Metal Ions"; Interrante, L. V., Ed.; American Chemical Society: Washington, DC, 1974; ACS Symp. Ser. No. 5, pp 94-107.
  (25) Hatfield, W. E. In "Extended Interactions between metal Ions"; In-
- terrante, L. V., Ed.; American Chemical Society: Washington, DC, 1974;
- ACS Symp. Ser. No. 5, pp 108-141.
  (26) Hopfield, J. J. In "Proceedings of the 29th International Congress of Societe de Chimie Physique, Orsay, 1976"; Roux, E., Ed.; Elsevier: Amsterdam, 1977; pp 417-430.
- (27) Siders, P.; Cave, R. J.; Marcus, R. A. J. Chem. Phys. 1984, 81, 5613-5624.
- (28) Levich, V. G.; Dogonadze, R. R. Collect. Czech. Chem. Commun. 1961, 26, 193-214 (translated by O. Boshko, University of Ottawa, Ontario, Canada).
- (29) Kestner, N. R.; Logan, J.; Jortner, J. J. Phys. Chem. 1974, 78, 2148-2166
  - (30) Ulstrup, J. Springer Lect. Notes Chem. 1979, 10.

<sup>&</sup>lt;sup>†</sup>California Institute of Technology.

University of Notre Dame. Present address: Florida Atlantic University. Contribution No. 7268.

<sup>&</sup>lt;sup>⊥</sup> Document No. NDRL-2749.

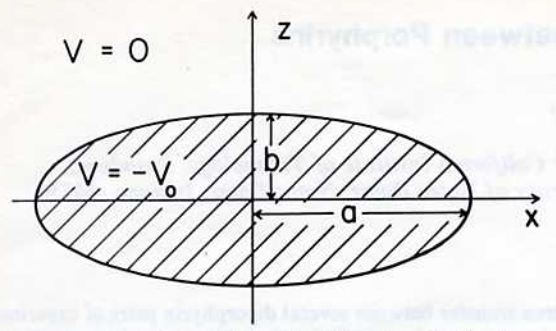


Figure 1. Potential well for a single site. There is cylindrical symmetry about the z axis.

potential shape on the rate of electron transfer at fixed distances and orientations. Such calculations, to the extents that they are applicable, can reveal ways in which the architecture of individual electron-transfer pairs may help control electron-transfer rates. In particular, orientation effects are examined for the forward reaction  $A^* + B \rightarrow A^+ + B^-$  for several systems,  $A^*$  denoting a photoexicted molecule, and for the highly exothermic reverse reaction  $A^+ + B^- \rightarrow A + B$ . The systems for which calculations are reported are (a) synthetic face-to-face porphyrins, including an open-jawed configuration, (b) porphyrin-like systems in an edge-to-edge configuration, (c) porphyrin systems comparing edge-to-edge and face-to-face as well as intermediate configurations, and (d) a photosynthetic system involving a dimeric photoexcited chlorophyll molecule.

The actual experimental results for which orientation effects have been explicitly studied are at present relatively few. In particular, there are the results of Chang et al.<sup>7-10</sup> and Overfield et al.<sup>11,12</sup> which are compared with the present results below.

The present article is organized as follows: The model is summarized and the methods of choosing states and energies for given systems are discussed in section II. Calculated results for several physical systems are given in section III, and they are discussed in section IV.

#### II. Theoretical Model

In current theories of nonadiabatic electron transfer<sup>28-30</sup> the rate constant for electron transfer between two reactants, A and B, at a given fixed separation distance and orientation is given by

$$k_{\rm B-A} = \frac{2\pi}{\hbar^2} |T_{\rm BA}|^2 \rm FC \tag{1}$$

In eq 1, FC is a sum of thermally weighted Franck-Condon factors for the nuclear vibrational, librational, and rotational coordinates of the two reactants and the surrounding medium.  $^{28\text{-}34}$  The distance and the orientation dependences of the rate constant occur mainly in the factor  $T_{\rm BA}$ , given by  $^{27,29,35}$ 

$$T_{\rm BA} = (H_{\rm BA} - S_{\rm AB}H_{\rm AA})/(1 - |S_{\rm AB}|^2)$$
 (2)

where

$$H_{\rm BA} = \langle \Psi_{\rm B} | H_{\rm A}' | \Psi_{\rm A} \rangle, \quad H_{\rm AA} = \langle \Psi_{\rm A} | H_{\rm A}' | \Psi_{\rm A} \rangle$$
 (3)

$$S_{AB} = \langle \Psi_A | \Psi_B \rangle \tag{4}$$

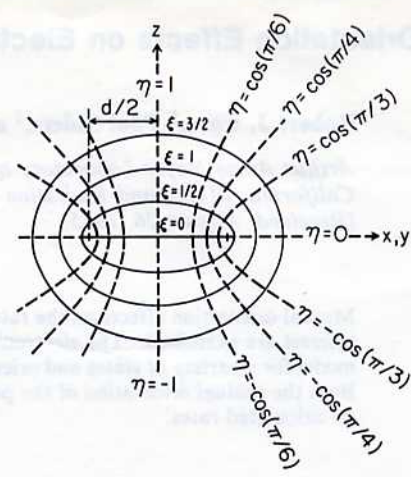


Figure 2. Oblate-spheroidal coordinate system. Contours of constant  $\xi$  are indicated by solid lines. The dashed lines are contours of constant  $\eta$ . The contours of constant  $\eta$  on the right are for  $\varphi=0$ , and those on the left are for  $\varphi=\pi$ .

The matrix element  $T_{\rm BA}$  has been calculated within a simple one-electron model<sup>27</sup> and examined as a function of reactant separation and orientation.  $\Psi_{\rm A}$  denotes the one-electron wave function associated with the electron being localized at site A in the absence of site B;  $\Psi_{\rm B}$  is analogously defined.  $H_{\rm A}'$  is the difference between the actual electronic Hamiltonian of the system and the Hamiltonian for site A. A detailed description of the model and wave functions is given in ref 27. Several elements are briefly reviewed below.

An oblate-spheroidal square well of constant depth was chosen to model the single-site potential experienced by the transferable electron localized at a molecule such as a porphyrin or quinone. The potential is illustrated in Figure 1. The plane of the molecule lies in the xy plane. The potential V is a negative constant,  $-V_0$ , inside the well and is zero outside. The single-site Hamiltonian is (in atomic units)

$$H_{\rm A} = -\frac{1}{2}\nabla^2 + V_{\rm A}$$
 (5)

With this Hamiltonian an energy E can be computed, given by  $\langle \Psi_A | H_A | \Psi_A \rangle$ . For the given value of  $V_A$  this E becomes a vertical one-electron ionization potential from the orbital  $\Psi_A$ .

Exact (three-dimensional) eigenfunctions were calculated for this Hamiltonian. Oblate-spheroidal coordinates<sup>36</sup>  $(\xi, \eta, \varphi)$  (Figure were used to solve the Schroedinger equation. The coordinate  $\varphi$  is the angle of rotation around the z axis. The wave function  $\Psi(\xi,\eta,\varphi)$  can be written as  $\Psi(\xi,\eta)\Phi(\varphi)$ . The Schroedinger equation can then be separated with respect to  $\varphi$ , and one obtains  $c_1$  cos  $m\varphi + c_2 \sin m\varphi$  for  $\Phi_m(\varphi)$ . The separation constant m depends on the given quantum state of interest. The function  $\Psi(\xi,\eta)$  is even or odd with respect to reflection in the xy plane. There are three types of possible nodal surfaces for Ψ, roughly corresponding to constant-coordinate surfaces for the three coordinates  $\xi$ ,  $\eta$ , and (exactly) φ. An ξ-type nodal surface is radial-like. (More precisely, at large distances  $d\xi/2$  is approximately equal to the distance from the center of the spheroid.) Wave functions with one  $\eta$ -type node have, by symmetry, the xy plane of the potential as a nodal surface; i.e., they have  $\pi$ -symmetry with respect to the xy plane. The  $\pi$ -like nature of such states is shown in Figures 3a and 4a. Higher numbers of  $\eta$ -type nodes are symmetrically placed about the xy plane. The  $\varphi$ -type nodal surfaces are planes through the origin, perpendicular to the molecular xy plane. Contour plots of states having m = 4 and m = 5 are given in Figures 3 and 4. In particular, Figures 3b and 4b are useful in visualizing the  $\varphi$ -type nodal surfaces.

When two oblate-spheroidal potential wells are chosen at a given separation distance and orientation, each with a specific single-site wave function, the various integrals in eq 3 and 4 can be evaluated

<sup>(31)</sup> Buhks, E.; Bixon, M.; Jortner, J.; Navon, G. Inorg. Chem. 1979, 18, 2014-2018.

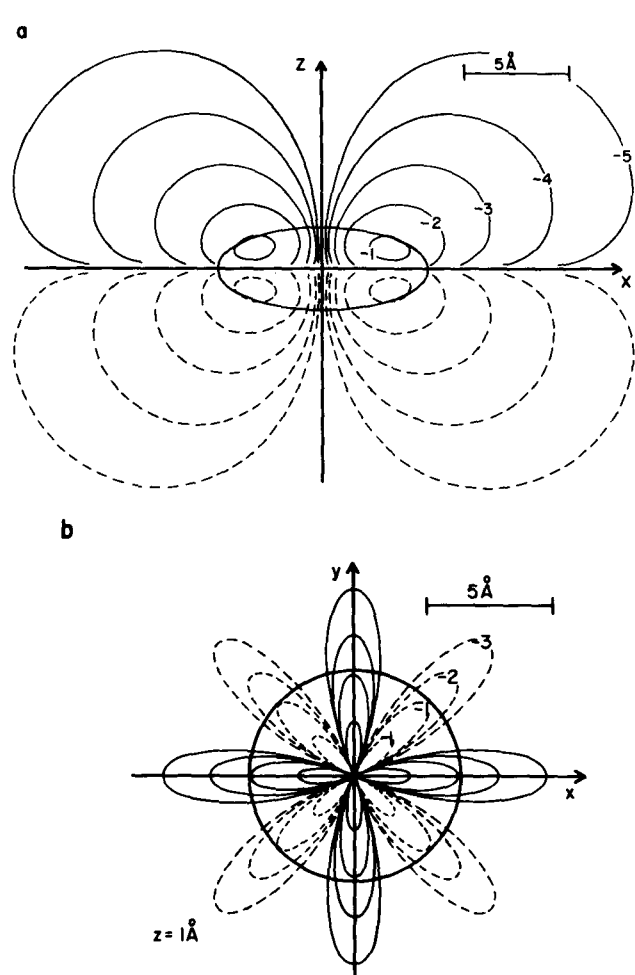
 <sup>(32)</sup> Siders, P.; Marcus, R. A. J. Am. Chem. Soc. 1981, 103, 741-747.
 (33) Siders, P.; Marcus, R. A. J. Am. Chem. Soc. 1981, 103, 748-752.

<sup>(34)</sup> Brunschwig, B. S.; Logan, J.; Newton, M. D.; Sutin, N. J. Am. Chem.

Soc. 1980, 102, 5798-5809.

<sup>(35)</sup> Incidentally, both the  $T_{\rm BA}$  and the  $H_{\rm BA}$  defined by eq 2 and 3 are independent of the zero of potential energy. In particular, if a constant C is added to the potential energy of the system, with  $V_{\rm A}$  and  $V_{\rm B}$  defined as in the text,  $H_{\rm A}$  is given by eq 5, but with C added to the right-hand side,  $H_{\rm B}$  is given by a similar equation with A replaced by B and H is given by  $-\nabla^2/2 + V_{\rm A} + V_{\rm B} + C$ . Thereby,  $H_{\rm A}'$  equals  $V_{\rm B}$  as before, and  $H_{\rm B}'$  equals  $V_{\rm A}$ . From eq 3 it is clear then that  $H_{\rm BA}$  is independent of the choice of C for the present model.

<sup>(36)</sup> Flammer, C. "Spheroidal Wave Functions"; Stanford University Press: Stanford, CA, 1957.



The contours are labeled with values of log  $|\Psi|$ . Dashed lines indicate  $\Psi < 0$ , and solid-line contours are for  $\Psi > 0$ . In (a) the contours shown are in the xz plane. In (b) the contours shown are in a plane parallel to the xy plane which intersects the z axis at z = 1 Å.

Figure 3. Contours of  $\Psi$  for a  $(4,\pi)$  state for  $V_0 = 19.2227$  eV, E = -0.4000 eV, a = 5 Å, and b = 2 Å. The heavy line is the well boundary.

and  $T_{BA}$  obtained. Since the total Hamiltonian for the system,

$$H_{\text{tot}} = -\frac{1}{2}\nabla^2 + V_A + V_B = H_A + V_B = H_B + V_A$$
 (6)

one has for the perturbation  $H_A'$  to  $H_A$ 

$$H_{A}' = V_{B} \tag{7}$$

Due to the definition of  $V_B$ , the expressions in eq 3 then reduce

$$H_{\rm BA} = -V_0^{\rm B} \langle \Psi_{\rm B} | \Psi_{\rm A} \rangle_{\rm B}, H_{\rm AA} = -V_0^{\rm B} \langle \Psi_{\rm A} | \Psi_{\rm A} \rangle_{\rm B} \tag{8}$$

where the subscript B on the integrals indicates that integration is only over well B. For the states used in the present article it was found in all cases that  $T_{BA}$  was equal to  $H_{BA}$  to within 3% when  $H_{BA}$  was nonzero and that the accuracy increased with separation distance.<sup>35</sup> Furthermore, for a pair of  $(4,\pi)$  states having the energy used in ref 27, it was found that the zeros of  $T_{\rm BA}$  and  $H_{\rm BA}$ , for the orientations of Figure 5d, were within two degrees of one another when the wells were in contact. Accordingly, only values of  $H_{BA}$  are presented in this paper. In Appendix A a method is shown for converting  $H_{RA}$  to a two-dimensional integral which reduces the computation time for  $H_{\rm BA}$ significantly. The numerical results are the same as those from the direct three-dimensional integration over well B and were used here. Conceptually, it is perhaps easier to envision the threedimensional integral, and for that reason, the discussion of the

results given below is in terms of the three-dimensional expression. The states chosen for a given calculation of  $H_{BA}$  are dependent upon the molecular system being modeled. Since the present

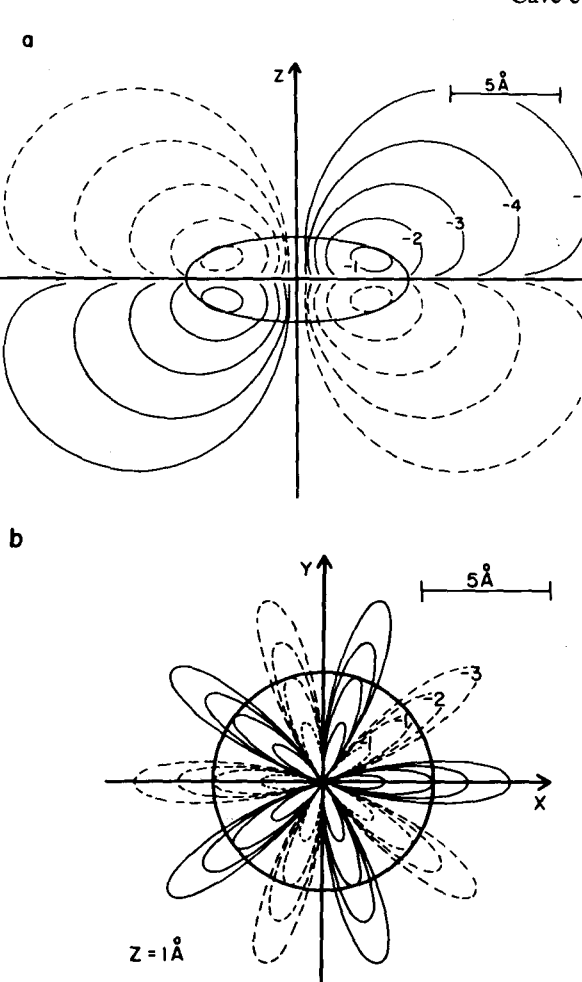


Figure 4. Contours of  $\Psi$  for a  $(5,\pi)$  state for  $V_0 = 23.4040$  eV, E =-0.4000 eV, a = 5 Å, and b = 2 Å. The labeling conventions of Figure 3 were followed.

article is concerned with electron transfers involving porphyrins and related compounds, the method of selecting the states appropriate to these systems is discussed. In all cases it is assumed that the transferable electron is delocalized over the porphyrin ring and does not have significant density on any central metal atom. A similar rationale could be applied to other cyclic aromatics.

In one early theoretical attempt to understand porphyrin spectra the  $\pi$ -electrons were treated as being confined to a one-dimensional ring.37 Within this treatment, the eigenfunctions are of the form  $\exp(\pm im\varphi)$ , the highest occupied pair of orbitals having m=4and the lowest unoccupied pair having m = 5.37 Later theoretical work by Gouterman<sup>38,39</sup> united the ring model description with a molecular orbital approach in what has become known as the "four-orbital model".39

The wave functions obtained in the molecular orbital approach<sup>40</sup> are real, the HOMO and HOMO - 1 resembling  $\cos 4\varphi$  and  $\sin$  $4\varphi$ , and the LUMO and LUMO + 1 resembling the cos  $5\varphi$  and  $\sin 5\varphi$ . Later ab initio calculations<sup>41-44</sup> have further supported

<sup>(37)</sup> Simpson, W. T. J. Chem. Phys. 1949, 17, 1218-1221.

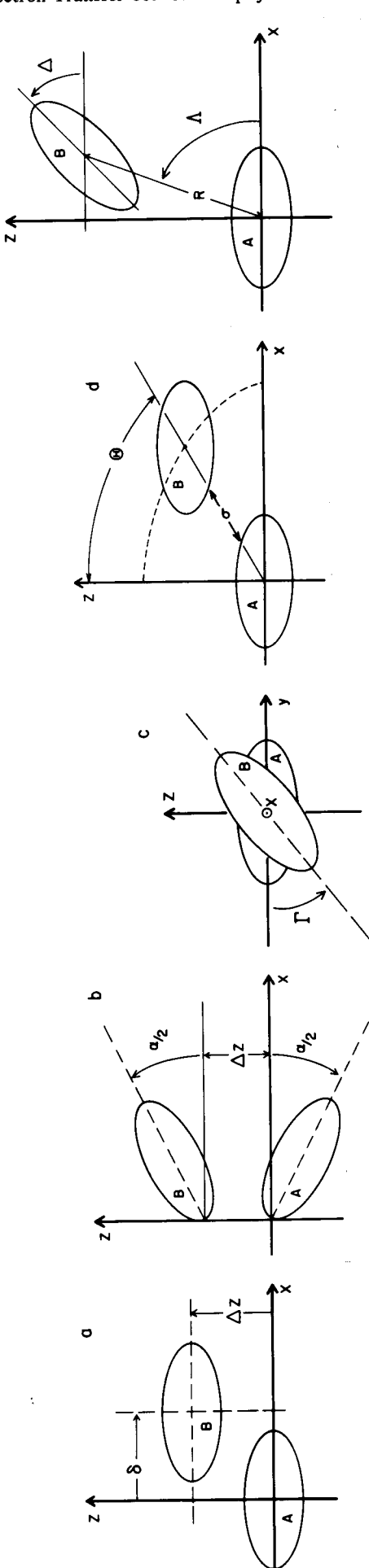
<sup>(38)</sup> Gouterman, M. In "The Porphyrins"; Dolphin, D., Ed.; Academic Press: New York, 1978; Vol. III, Chapter 1.

<sup>(39)</sup> Gouterman, M. J. Mol. Spectrosc. 1961, 6, 138-163.
(40) Longuet-Higgins, H. C.; Rector, C. W.; Platt, J. R. J. Chem. Phys. 1950, 18, 1174-1181.

<sup>(41)</sup> Spangler, D.; Maggiora, G. M.; Shipman, L. L.; Christoffersen, R. E. J. Am. Chem. Soc. 1977, 99, 7470-7477.

<sup>(42)</sup> Spangler, D.; Maggiora, G. M.; Shipman, L. L.; Christoffersen, R. E. J. Am. Chem. Soc. 1977, 99, 7478-7489.

<sup>(43)</sup> Christoffersen, R. E. Int. J. Quantum Chem. 1979, 16, 573-604.
(44) Petke, J. D.; Maggiora, G. M.; Shipman, L. L.; Christoffersen, R. E. Photochem. Photobiol. 1979, 30, 203-223.



separation,  $\Delta z$ . (b) Orientations examined in Figure 8. (c) End-on view of the mutual orientations of the xy planes of the two wells for which results are presented in Figure 9. The value  $\Gamma = 0^{\circ}$  corresponds to the z axes of the wells are parallel and lie in the plane of the figure in all geometries.  $\theta = 0^{\circ}$  corresponds to the z axes of the wells being parallel. (d) Orientations examined in Figures 10 and 11. z axes of the wells being parallel. (d) Orientations examined in Figures 10 and 11. The x axes of the wells are parallel and lie in the plane of the figure in all geometries. Θ = 0° corresponds to the z axes of the wells lying along the same line. σ is the edge-to-edge separation distance. (e) Coordinate system used to describe the results presented in Figures 12 and 13. The x axes of the wells are in the plane of the figure. Figure 5. Relative orientations of the diporphyrin systems examined in the present article. (a) Orientations examined in Figures 6 and 7.  $\delta = 0$  corresponds to the z axes lying on a common line at a given interplane R is the center-to-center separation distance. the general predictions of the four-orbital model as to the shapes of the four orbitals and their energetic separation from other states.

In this article, states with one  $\eta$ -type node (which are  $\pi$ -states) and with m = 4 or 5 (designated  $(4,\pi)$  and  $(5,\pi)$ , respectively) were chosen to qualitatively reproduce the four-orbital model states. Figures 3 and 4 show contour plots of  $(4,\pi)$  and  $(5,\pi)$ states. The nodal patterns are qualitatively similar to those of the HOMO and LUMO orbitals in ab initio calculations for porphyrin-like molecules.<sup>41-43</sup> Metallo- and free-base porphyrins, chlorophylls, and bacteriochlorophylls were all treated as having the same HOMO's and LUMO's.

In modeling the first excited singlet state of a given molecule, one only considers the excited, transferable electron. The fourorbital model<sup>38,39</sup> predicts that the first excited singlet state is composed of linear combinations of pairs of the possible primitive excitations formed from the four orbitals of interest. The extent of mixing of the possible single excitations will determine the fraction of mixing of cos  $5\varphi$  and  $\sin 5\varphi$  in the donor wave function (cf. ref 38, 39, and Appendix B). This mixing will depend on the symmetry, substituents, and the environment of the molecule. Using the four-orbital model and semiempirical<sup>38</sup> or ab initio<sup>44</sup> molecular orbital calculations, we could estimate the extent of mixing between the pair of single excitations which make up the first excited singlet state, thus yielding an approximate description of a given excited state within the present model (see Appendix B). However, the results below are presented for  $\Phi_m(\varphi) = \cos \varphi$  $5\varphi$  or  $\sin 5\varphi$  to ensure that the orientation effects seen are not peculiar to a specific choice of  $\Phi_m(\varphi)$ . Any  $\Phi_m(\varphi)$  can be generated as a linear combination of the above.

To represent the HOMO of a (metallo)porphyrin anion  $\Phi_m$  =  $\cos 5\varphi$  or  $\sin 5\varphi$  was again chosen, on the assumption that the additional electron is placed in the LUMO of the neutral molecule. ESR data on bacteriochlorophylls (BChl) and bacteriopheophytins (BPh) indicate that the unpaired spin density is delocalized over the entire ring.<sup>45</sup> The spin densities obtained from ab initio<sup>46</sup> and semiempirical calculations<sup>45</sup> are in reasonable agreement with experimental results and can be approximately described as having the extra electron in the LUMO of the neutral molecule. 46

Finally, in modeling the empty orbital in (metallo)porphyrin cations, we selected  $\Phi_m(\varphi) = \cos 4\varphi$  or  $\sin 4\varphi (4,\pi)$  states. Evidence from comparisons of MO calculations with ESR measurements on porphyrins suggests that these cations can be described qualitatively by such localized, single-electron hole descriptions.<sup>45</sup> In the case of certain metalloporphyrins only a few percent of the electron density is delocalized on the porphyrin ring. The present results are not applicable, therefore, to transfers through heme faces. It is possible that the calculations are still applicable to transfer through heme edges, but with appropriately reduced values of the matrix elements  $T_{\rm BA}$ .

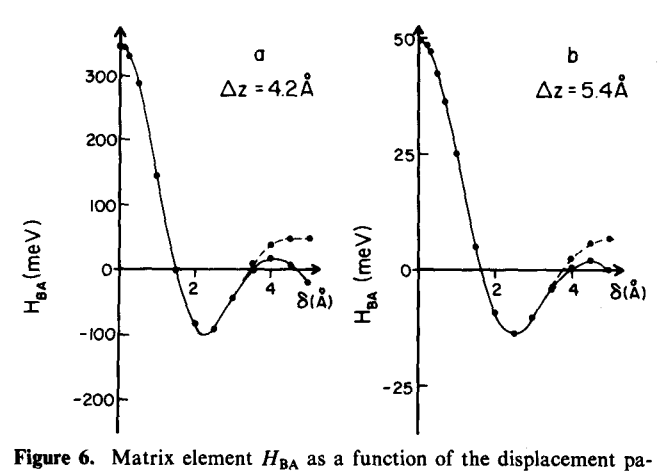
In summary, in the results of the following section  $H_{BA}$  is examined as a function of orientation for transfer of an electron initially localized in a  $(5,\pi)$  state transferring to a  $(5,\pi)$  state of the acceptor  $[(5,\pi) \rightarrow (5,\pi)]$  and for transfer of an electron initially localized in a  $(5,\pi)$  orbital transferring to a  $(4,\pi)$  state,  $[(5,\pi) \rightarrow (4,\pi)]$ . The  $(5,\pi) \rightarrow (5,\pi)$  transfer can be viewed as "forward transfer" between a photoexcited molecule and a neutral acceptor. The  $(5,\pi) \rightarrow (4,\pi)$  transfer can be viewed as "back transfer" from a reduced acceptor to an oxidized donor to yield the ground-state species.

The sizes of the potential wells were chosen as follows. The semimajor axis a was chosen as 5 Å, an approximate in-plane radius of the porphine system.<sup>47</sup> The semiminor axis b was chosen as 2 Å. This  $\dot{b}$  yields an average thickness of 2.7 Å for the spheroidal well.<sup>27</sup> This value represents approximately the "thickness" of the electron cloud obtained from ab initio calculations on a substituted porphyrin<sup>42</sup> and allows approach of the "molecular" planes to distances close to those found in synthetic

<sup>(45)</sup> Fajer, J.; Davis, M. S. In "The Porphyrins"; Dolphin, D., Ed.; Academic Press: New York, 1979; Vol. IV, Chapter 4.

<sup>(46)</sup> Petke, J. D.; Maggiora, G. M.; Shipman, L. L.; Christoffersen, R. E. Photochem. Photobiol. 1980, 32, 399-414; 1981, 33, 663-671.

<sup>(47)</sup> Webb, L. E.; Fleischer, E. B. J. Am. Chem. Soc. 1965, 87, 667-669.



rameter  $\delta$  defined in Figure 5a at two fixed interplane separations for  $(5,\pi) \rightarrow (5,\pi)$  transfer; (a) interplane spacing = 4.2 Å; (b) interplane spacing = 5.4 Å. For the donor and acceptor states a, b, E, and  $V_0$  were as in Figure 4. The solid line indicates  $\Phi_m(\varphi) = \cos m\varphi$  in each well; the dashed line indicates  $\Phi_m(\varphi) = \sin m\varphi$  in each well:

systems. 7,48,49 As in ref 27, the trends in the results presented on orientation dependence are not sensitive to the exact values of a and b.

The energy E was chosen to make the decay of  $H_{BA}$  with separation distance lie in the general vicinity of a number of experimental estimates.  $^{50-53}$  In ref 27 it was shown that  $H_{\rm BA}(R)$ in the present model decayed approximately exponentially with increasing separation of the wells. The calculated decay constant  $\beta$  for  $|H_{BA}|^2$  depends on the range of distances for  $H_{BA}$  being used, since  $H_{BA}$  is not a pure exponential. Here, the estimated  $\beta$ 's were obtained for edge-to-edge separations of between 10 and 20 Å since several experimental studies have produced estimates of  $\beta$  for transfers at these distances. 53,54 (Such distances are appropriate to those estimated in studies of tunneling in glassy matrices.) In general, the calculated  $\beta$  decreases with increasing distance between the wells. The calculated  $\beta$  also depends on the orientation of the wells. The orientations chosen for estimating  $\beta$  were those of Figure 5d. The angles  $\theta = 0^{\circ}$ ,  $60^{\circ}$ , and  $90^{\circ}$  were

chosen as representative;  $\theta = 60^{\circ}$  approximately corresponds to the maximum in  $H_{BA}$  as a function of  $\theta$  for a given edge-to-edge distance for this class of orientations. We have chosen E = -0.400eV which, for  $(5,\pi) \rightarrow (5,\pi)$  transfer, yields  $\beta$ 's of 1.5, 1.4, and 1.3 Å<sup>-1</sup> for  $\theta$  = 0°, 60°, and 90°, respectively, over the above range of distances. Since  $\theta = 60^{\circ}$  corresponds to the maximum in  $H_{BA}$ for the class of orientations, its decay should be most important in determining  $\beta$  when averaged over  $\theta$ . Other orientations may yield different  $\beta$ 's, but they are expected to fall in the range of the above values. In electron-transfer reactions, the energy region of interest is

that near the intersection of the reactants' and products' potential energy surfaces,55 i.e., at the transition state for the reaction. In this region the reactants' and products' electronic energies are equal. The donor and acceptor potential depths were thus adjusted to make the energies of  $\Psi_A$   $(E_A = \langle \Psi_A | H_A | \Psi_A \rangle)$  and  $\Psi_B$   $(E_B =$  $(\Psi_B|H_B|\Psi_B)$ ) equal to -0.400 eV, for both forward and reverse transfer. The relative angular dependence is largely unaffected by the orbital energies used.

(55) (a) Marcus, R. A. J. Chem. Phys. 1965, 43, 679-701. (b) Marcus, R. A. J. Chem. Phys. 1970, 52, 2803-2804.

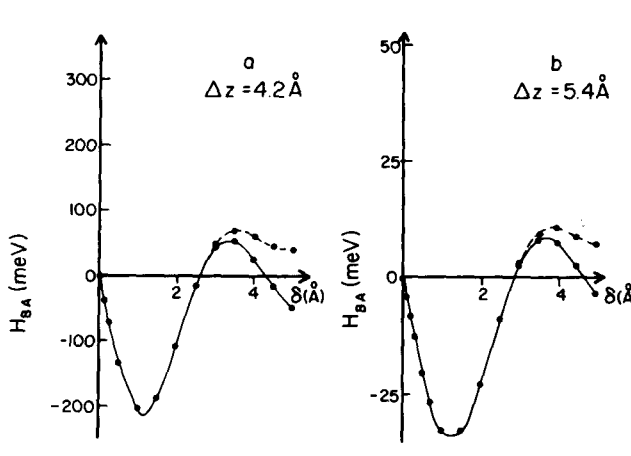


Figure 7. Matrix element  $H_{BA}$  as a function of the displacement parameter  $\delta$  defined in Figure 5a at two fixed interplane separations for  $(5,\pi) \rightarrow (4,\pi)$  transfer: (a) interplane spacing = 4.2 Å; (b) interplane spacing = 5.4 Å. For the donor and acceptor states a, b, and E were as in Figure 4. For the donor,  $V_0$  was as in Figure 4, and for the acceptor,  $V_0$  was in Figure 3. The labeling convention of Figure 6 was used.

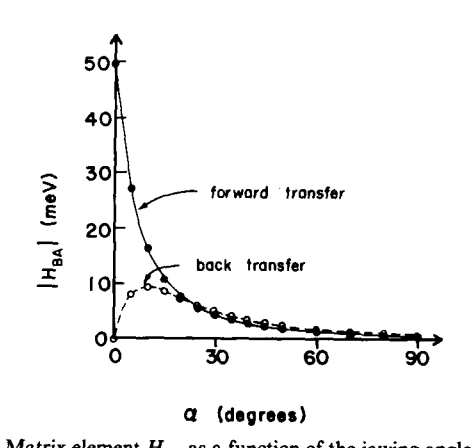


Figure 8. Matrix element  $H_{\rm BA}$  as a function of the jawing angle  $\alpha$  defined in Figure 5b between the two porphyrin planes. For forward transfer  $((5,\pi) \rightarrow (5,\pi))$  the states used were as in Figure 6. For back transfer  $((5,\pi) \rightarrow 4,\pi)$ ) the states used were as in Figure 7. In both cases initial and final states were of the form  $\cos m\varphi$ .

### III. Results

Results are presented in this section for the set of orientations depicted in Figure 5. In Figure 5a the xy planes of the two wells are assumed parallel, and  $\delta$  is the distance between the z axes of the two wells along their common x direction. The orientations in Figure 5b involve a jawing motion of the two porphyrins through the angle  $\alpha$ , the xy planes of the wells being parallel at  $\alpha = 0^{\circ}$ . The interplane separation at the assumed hinge point is fixed at the value  $\Delta z$ . The orientations described in Figure 5c involve an edge-to-edge configuration of the wells. The wells are first translated relative to one another along their common x axis, and then one well is tilted through an angle  $\Gamma$  as shown in Figure 5c. The edge-to-edge distance along the common x axis for the orientations of Figure 5c is denoted by the parameter d (not shown). The orientations in Figure 5d involve wells with parallel xy planes, with the origin of the second well moved through the swing angle  $\Theta$ . The parameter  $\sigma$  is the edge-to-edge separation distance. In Figure 5e, a set of orientations used to examine possible electronic effects in bacterial photosynthetic reaction centers is shown.

Values of  $H_{BA}$  are plotted in Figures 6 and 7 for the  $(5,\pi) \rightarrow$  $(5,\pi)$  and  $(5,\pi) \rightarrow (4,\pi)$  transfers, respectively, between two porphyrins held at a fixed interplane separation distance. The results are presented as a function of the displacement parameter  $\delta$  defined in Figure 5a. The xy planes are held at 4.2 Å in Figures 6a and 7a and at 5.4 Å in Figures 6b and 7b. These distances were chosen to model the interplane separations of the compounds of Chang.7

<sup>(48)</sup> Collman, J. P.; Chong, A. O.; Jameson, G. B.; Oakley, R. T.; Rose, E.; Schmittou, E. R.; Ibers, J. A. J. Am. Chem. Soc. 1981 103, 516-533 (49) Hiom, J.; Paine III, J. B.; Zapf, U.; Dolphin, D. Can. J. Chem. 1983, 61, 2220-2223.

<sup>(50)</sup> Alexandrov, I. V.; Khairutdinov, R. F.; Zamaraev, K. I. Chem. Phys. 1978, 32, 123-141

<sup>(31)</sup> Beitz, J. V.; Miller, J. R. J. Chem. Phys. 1979, 71, 4579-4595.
(52) Miller, J. R.; Beitz, J. V. J. Chem. Phys. 1981, 74, 6746-6756. (53) Strauch, S.; McLendon, G.; McGuire, M.; Guarr, T. J. Phys. Chem.

<sup>(54)</sup> Miller, J. R.; Hartman, K. W.; Abrash, S. J. Am. Chem. Soc. 1982, 104, 4296-4298.

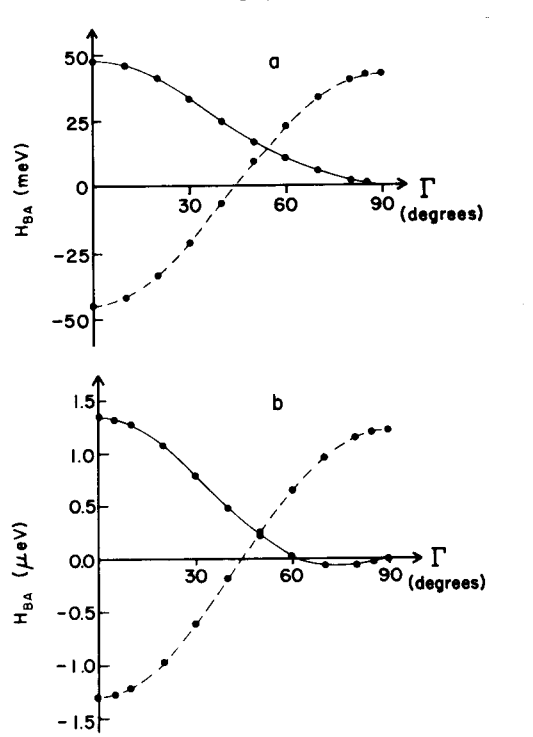


Figure 9. Matrix element  $H_{\rm BA}$  as a function of the twist angle  $\Gamma$  defined in Figure 5c at several fixed edge-to-edge separations for  $(5,\pi) \to (5,\pi)$  transfer: (a) edge-to-edge separation = 0 Å (i.e., contact); (b) edge-to-edge separation = 10 Å. For the donor and acceptor states,  $a, b, V_0$ , and E were as in Figure 4. The solid and dashed lines have the same meaning as those of Figure 6.

Calculations of  $H_{BA}$  for  $(5,\pi) \to (5,\pi)$  and  $(5,\pi) \to (4,\pi)$  transfers are given in Figure 8 as functions of the jawing angle  $\alpha$  between the porphyrin planes (Figure 5b). In Figure 9,  $H_{BA}$  is presented as a function of  $\Gamma$  at two different d values for the orientations shown in Figure 5c. Values of  $H_{BA}$  calculated for the orientations of Figure 5d are presented in Figures 10 and 11.  $H_{BA}$  is shown in Figure 10 as a function of  $\Theta$  for the  $(5,\pi) \to (5,\pi)$  transfer for two different edge-to-edge separations. Analogous results for the  $(5,\pi) \to (4,\pi)$  transfer are shown in Figure 11. The class of orientations considered in Figure 5e may be regarded as pertinent to the relative orientation of the special pair dimer and the BChl b monomer, as given in the recent reaction center crystal structure of *Rhodopseudomonas viridis*. In modeling electron transfer between these centers, it is assumed

that the excited transferable electron is delocalized over a linear combination of the LUMO's of the two molecules which constitute the dimer. (In fact, its initial identification was based upon measurements indicating this delocalization.<sup>1</sup>) Since each BChl b monomer is closely associated with only one of the two molecules in the dimer, it was assumed for simplicity that  $H_{\rm BA}$  need only be calculated between the closest member of the dimer and the BChl b.<sup>56</sup>

 $H_{\rm BA}$  as a function of  $\Delta$ , with  $\Lambda = \Delta$ , is shown in Figure 12 for both the  $(5,\pi) \to (5,\pi)$  and the  $(5,\pi) \to (4,\pi)$  transfers. The experimental data<sup>6</sup> indicate that there is a 70° angle between donor and acceptor ring planes in the above system. The experimental orientation is approximated here by setting  $\Delta = \Lambda = 70^{\circ}$ . In Figure 13,  $\Delta$  is held fixed at 70° and  $\Lambda$  is varied from 30° to 90°.

## IV. Discussion

The results of the previous section are considered here in the order presented there.

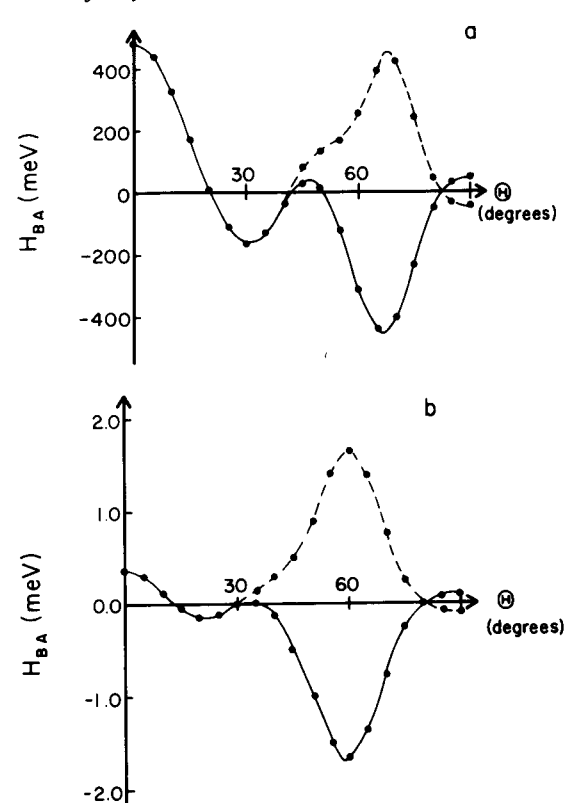


Figure 10. Matrix element  $H_{\rm BA}$  as a function of  $\theta$  defined in Figure 5d at several fixed edge-to-edge separations for  $(5,\pi) \to (5,\pi)$  transfer: (a) edge-to-edge separation = 0 Å (i.e., contact); (b) edge-to-edge separation = 5 Å. For the donor and acceptor states, a, b, E, and  $V_0$  were as in Figure 4. The labeling convention of Figure 6 was used for solid and

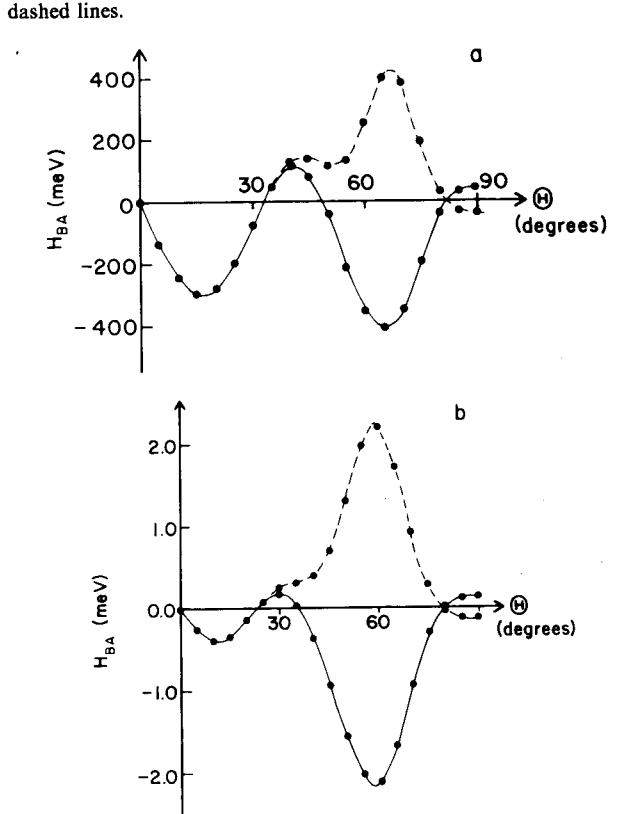


Figure 11. Matrix element  $H_{\rm BA}$  as a function of  $\theta$  defined in Figure 5d at several fixed edge-to-edge separations for  $(5,\pi) \to (4,\pi)$  transfers: (a) edge-to-edge separation = 0 Å (i.e., contact); (b) edge-to-edge separation = 5 Å. For the donor and acceptor states, a, b, and E were as in Figure 3. For the donor  $V_0$  was as in Figure 4, and for the acceptor,  $V_0$  was as in Figure 3. The conventions of Figure 6 for solid and dashed lines were followed in labeling the results.

<sup>(56)</sup> On the basis of recent optical evidence [Meech, S. R.; Hoff, A. J.; Wiersma, D. A. Chem. Phys. Lett. 1985, 121, 287-292] it has been proposed that the initial excitation of the BChl dimer is followed immediately (~0.025 ps) by the formation of an intramolecular charge-transfer state of the dimer. Subsequent charge transfer, e.g., to the BChl monomer, could then involve a transfer from the anion in the dimer.

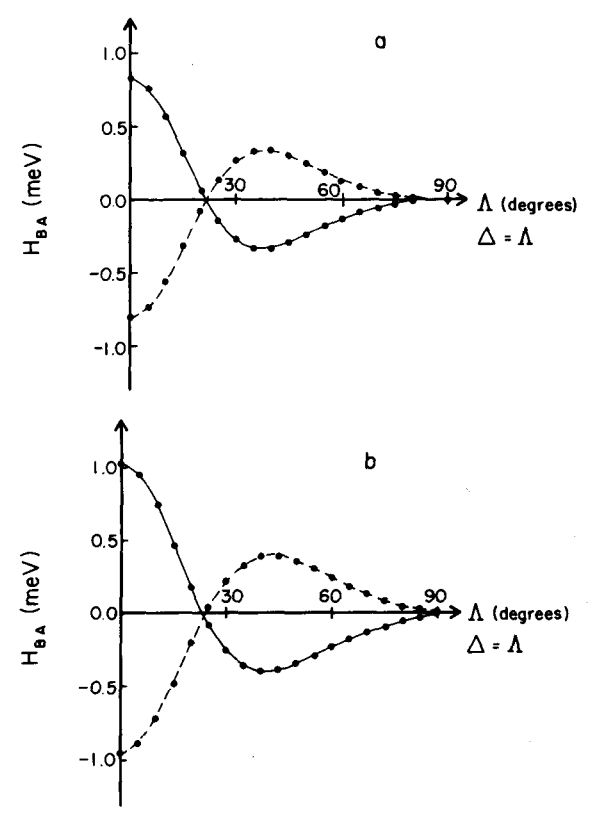


Figure 12. Matrix element  $H_{\rm BA}$  as a function of  $\Delta$  for  $\Delta = \Lambda$  where  $\Delta$  and  $\Lambda$  are defined in Figure 5c. The center-to-center separation is 13 Å. For both donor and acceptor states a, b, and E were as in Figures 3 and 4. The labeling convention of Figure 6 was used for solid and dashed lines. (a)  $(5,\pi) \to (5,\pi)$  transfer.  $V_0$  was as in Figure 4 for donor and acceptor states. (b)  $(5,\pi) \to (4,\pi)$  transfer.  $V_0$  was as in Figure 4 for the donor and as in Figure 3 for the acceptor.

In Figures 6 and 7 it is seen that the shapes of the  $H_{\rm BA}$  vs.  $\delta$ plots are generally similar at the two interplane separations. For the  $(5,\pi) \rightarrow (5,\pi)$  transfer in Figure 6 the maximum in  $|H_{BA}|$ occurs at  $\delta = 0$  Å with secondary maxima near  $\delta = 2$  and 4 Å, while the  $(5,\pi) \rightarrow (4,\pi)$  results in Figure 7 show a zero for  $|H_{BA}|$ at  $\delta = 0$  Å and local maxima near  $\delta = 1$  and 3.5 Å. This difference between forward (Figure 6) and back (Figure 7) transfer near  $\delta = 0$  Å is purely an orbital shape effect, due to the orthogonality of the  $\Phi_m(\varphi)$  functions for m = 4 and m = 5 in the face-to-face configuration. When the z axes of the two wells lie along a common line, the product  $\Phi_4(\varphi_A)\Phi_5(\varphi_B)$  vanishes by symmetry when integrated over  $\varphi_A$ . (Note that the integration is over well A in this case since back transfer occurs from B to A.) This large difference in forward and reverse matrix elements is very orientation dependent: Comparing Figures 6 and 7, it is seen that the forward and back transfer  $H_{BA}$ 's become of comparable magnitude for  $\delta > 3$  Å. The existence of a zero of  $H_{\rm BA}$  at  $\delta = 0$  applies also, exactly, to  $T_{\rm BA}$ , as one can show by a symmetry argument. The same remark applies for the back transfer results at  $\alpha = 0$  in Figure 8 given below.

Experimental results on such face-to-face porphyrins appear to indicate<sup>8-10</sup> fast, light-driven forward electron transfer (<6 ps) with slow back transfer to yield ground-state products ( $\sim$ 1 ns). It has been suggested that the back transfer is slow due to a large avoided crossing of the electronic surfaces, <sup>10</sup> which can occur in the inverted region, <sup>55b,57</sup> or because of the large driving force and small activation energy of the process, i.e., the "inverted effect", <sup>55</sup> or both. The results of Figures 6 and 7 indicate that an orbital

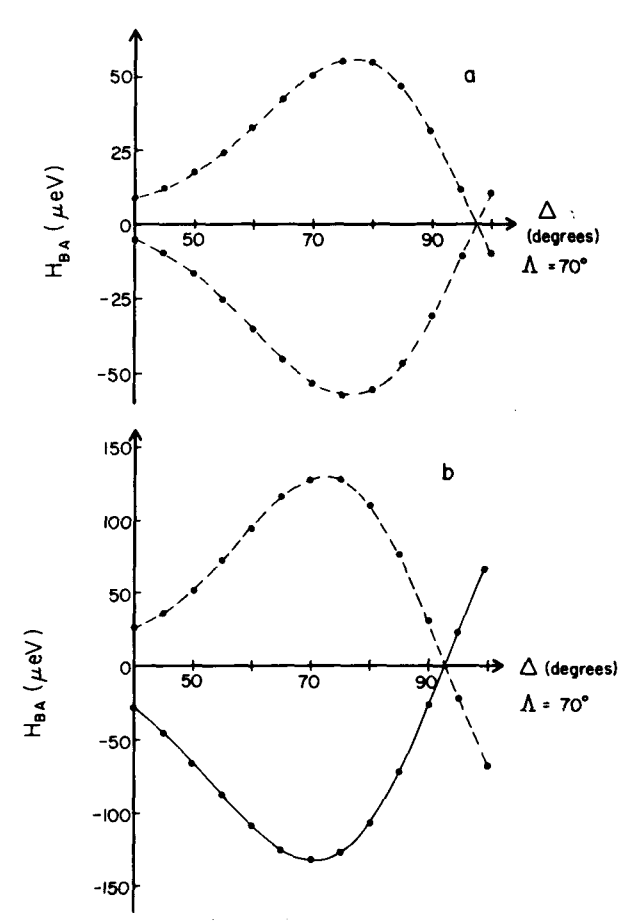


Figure 13. Matrix element  $H_{\rm BA}$  as a function of  $\Lambda$  for  $\Delta=70^{\circ}$  where  $\Delta$  and  $\Lambda$  are defined in Figure 5c at a center-to-center separation R of 13 Å. The states and conventions used are those of Figure 12. (a)  $(5,\pi)$   $\rightarrow (5,\pi)$  transfer. (b)  $(5,\pi) \rightarrow (4,\pi)$  transfer.

orientation effect could also contribute to the difference in rates in this face-to-face configuration.

The results given in Figure 8 show a dramatic dependence of  $H_{\rm BA}$  on the jawing angle  $\alpha$  for face-to-face porphyrins. For the  $(5,\pi) \to (5,\pi)$  and  $(5,\pi) \to (4,\pi)$  transfers it is seen that only for values of  $\alpha$  less than 20° are the forward and back transfer  $H_{\rm BA}$  signficantly different. For larger jawing angles the forward and back transfer  $H_{\rm BA}$ 's are virtually the same.

While there are no experimental results for the jawed configurations in Figure 5b, there are the results of Overfield et al. 11,12 for a somewhat different set of jawing configurations. In these studies evidence was obtained that suggests that forward and back transfer occur at essentially the same rate in the jawing diporphyrins studied, each state having a lifetime of  $\sim 1$  ns. This result is quite interesting because the interplane separation in this compound is comparable to that in the compounds of Chang, 8-10 and for small jawing angles, the molecules are coplanar. Such slow forward and back transfer may also be due to an orbital orientation effect. The compound examined by Overfield et al. 11,12 is a jawing diporphyrin, similar to that of Figure 5c, except that one of the wells is rotated 180° about a line in the xy plane of the potential which bisects the angle between the +x and +y axes. (Thus, the z axes of the wells are antiparallel, while the x(y) axis of well A is parallel to the y(x) axis of well B when the jawing angle is 0°.) If both the excited state of the donor and the acceptor state can be approximately described as the same single-configuration states (see Appendix B), a slow forward rate would be expected due to an electronic orientation effect, even when the jawing angle is small and the porphyrins are face-to-face, as in the Chang compounds. With  $\Phi_m(\varphi) = \cos m\varphi$  in each well, both the  $(5,\pi) \rightarrow (5,\pi)$  and  $(5,\pi) \rightarrow (4,\pi)$  transfers would yield zeros for  $H_{BA}$ . (Calculations are not shown since both transfers yield  $H_{\rm BA} = 0$ .) This feature is again an orbital shape effect peculiar to this class of orientations and results from the orthogonality of

<sup>(57)</sup> In the event that the reaction is nonadiabatic in both the forward and reverse directions, this avoided crossing in the inverted region will not cause any greater decrease in the rate than does the nonadiabaticity (i.e., the small splitting) in the normal region. In this case the major difference between forward and reverse rates would be due to the inverted effect rather than the avoided crossing.

Electron Transfer between Porphyrins

orbital orientation effect.

earlier.27

photosynthesis.

with the intermediate BChl b.

the  $\Phi_m(\varphi)$ 's. In the rotated configuration,  $\varphi_B = 1/2\pi - \varphi_A$ , so that  $\cos 5\varphi_{\rm B} = \sin 5\varphi_{\rm A}$ , which is itself orthogonal to  $\cos 5\varphi_{\rm A}$ . For nonzero jawing angles  $H_{BA}$  is still predicted to be zero for both forward and back transfer within the present model. To obtain a zero forward transfer matrix element for this class

of orientations for the compounds of Overfield et al.11,12 within the present model, it is necessary that the initially excited donor state be well characterized by a single-excitation wave function. To the extent that this is not true, the present model would predict a nonzero forward transfer matrix element. The high intensity of the Q bands in the spectra of ref 11 leads one to expect a largely single-configuration excited state for the compounds studied there on the basis of the four-orbital model.39 Therefore, the results of Overfield et al., 11,12 regarding the slow forward rate of transfer as compared to the compounds of Chang,7 may arise from an

systems having the orientations of Figures 5c and 5d, corresponding to the results presented in Figures 9-11. In the results of Figure 9, in which an edge-to-edge orientation was considered, it is seen that the shape of the  $H_{\rm BA}$  vs.  $\Gamma$  plot is relatively unaffected by an increase in separation distance, although  $H_{\rm BA}$  itself rapidly decreases with this distance. In the calculations presented in Figures 10 and 11,  $H_{\rm BA}$  is

At present there are apparently no experimental results for

examined at fixed edge-to-edge separations as a function of the angle  $\theta$ . The plots for both the  $(5,\pi) \to (5,\pi)$  and  $(5,\pi) \to (4,\pi)$ transfers exhibit several zeros and maxima between  $\theta = 0^{\circ}$  and  $\theta = 90^{\circ}$ . At  $\theta = 0^{\circ}$  the forward transfer  $H_{BA}$  shows a relative maximum while the back transfer  $H_{BA}$  is zero, the explanation being that given for the  $\delta = 0$  results of Figures 6 and 7. The orbital shape effect responsible for the difference in forward and back transfer  $H_{\rm BA}$ 's for a face-to-face orientation ( $\Theta = 0^{\circ}$ ) is not operative in the edge-to-edge configuration ( $\theta = 90^{\circ}$ ). The results illustrate the sensitivity of  $H_{BA}$  not only to the states involved in the transfer but also to the molecular orientation. The change

in relative size of the several maxima in Figures 10 and 11 as a

function of separation distance can be qualitatively understood

on the basis of orbital shape arguments similar to those given

The orientations examined in Figures 12 and 13 are of interest

to discussions of forward and reverse electron transfer in bacterial photosystems. For the approximate experimental geometry<sup>6</sup> ( $\Delta$ =  $\Lambda$  = 70°) the back transfer matrix element is more or less comparable in magnitude to that for forward transfer. Figure 13 indicates that no appreciable lowering of  $H_{BA}$  for back transfer relative to that for forward transer can be obtained by the change in orientation examined there. In the present model, therefore, there is no indication of electronic effects which would control the relative rates of forward and back electron transfer between

the initial donor and the nearest BChl b monomer in bacterial

Other factors may then be responsible for the control of the relative forward and reverse rates in this photosynthetic system as discussed earlier, for instance the inverted effect.55 These back electron transfers are excellent candidates for obtaining an inverted effect, due to the expected low reorganization energies 7-10 and the high driving forces. Also, the exact role of the BChl b in transfer to the adjacent BPh has not been unambiguously established. It is possible that the BPh is involved in the initial electron transfer, in which case the orientations of all three compounds should be considered, perhaps within a superexchange mechanism, 20,21,58,59

in  $H_{BA}$  as a function of the variation of a given orientational parameter. To the extent that the  $\pi$ -orbitals of the actual systems have shapes similar to the model wave functions used here and to the extent that many-electron effects can be neglected, qual-

In general, the present results exhibit several maxima and zeros

1584-1594.

itative agreement of more elaborate theoretical studies with the present results can be expected. However, some deviations from the actual positions of the maxima would not be unexpected.

We have noted that the present one-electron model predicts a large difference in forward and back transfer  $H_{BA}$ 's in the face-to-face configuration. It is useful to inquire how model dependent this is. In  $D_{4h}$  and  $D_{2h}$  porphyrins, the HOMO and LUMO are predicted to belong to a different irreducible representation of the molecular point group38,42,43 and thus will be orthogonal in the face-to-face configuration not only for the present wave functions but also for more detailed ones. If the actual many-electron potential can be approximated by a reasonably smooth one, then it would be expected that back transfer would again be predicted to be slow by using these more detailed wave functions in the face-to-face configuration. Deviations from  $D_{4h}$ or  $D_{2h}$  symmetry do not appear to affect the general shape of the HOMO or LUMO orbitals in ab initio calculations, 41-43 so it is

reasonable to expect that this particular prediction for the faceto-face configuration is not highly model dependent. It might appear from eq 8 that  $H_{BA}$  depends on the experimental "tail" of  $\Psi_A$  but not on that of  $\Psi_B$ . However, it actually depends on the latter, albeit indirectly, via the V<sub>B</sub> appearing in that equation.  $H_{\rm BA}$  can also be written equivalently as  $-V_0^{\rm A}\langle\Psi_{\rm A}|\Psi_{\rm B}\rangle_{\rm A}$ for the present case, where  $\langle \Psi_A | H_A | \Psi_A \rangle = E = \langle \Psi_B | H_B | \Psi_B \rangle$ .

The medium between two reactants is sometimes ordered and

sometimes disordered. While medium effects can be considered as included in the present model via the adjustment of E to yield a given value of  $\beta$ , the detailed effects of such environments on modifying, in a superexchange mechanism, the broad picture of the relative orientation effects described in this paper have not been examined. The general effects are expected to persist nevertheless. Clearly, experimental results when they become available will be particularly helpful in defining the practical utility of the present model and its predictions. V. Conclusions

## Calculations were reported for mutual orientation effects in electron transfers in diporphyrin systems. The donor and acceptor

states were modeled by using one-electron eigenfunctions of oblate-spheroidal wells. A variety of orientations were examined, and it was shown that the thermal matrix element for electron transfer is a highly sensitive function of orientation and the orbitals involved in the transfer. As more experimental results on such systems become available, the validity of the present predictions can be assessed. Acknowledgment. It is a pleasure to acknowledge support of

this research by the Office of Naval Research and by the Office of Basic Energy Sciences of the U.S. Department of Energy. R.J.C. gratefully acknowledges the support of a National Science Foundation Predoctoral Fellowship, 1979-1982. The calculations reported in this paper were made using the computational facilities of the Notre Dame Radiation Laboratory and, at Caltech, of the Dreyfus-NSF theoretical chemistry computer which was funded through grants from the Camille and Henry Dreyfus Foundation, the National Science Foundation, and the Sloan Fund of the California Institute of Technology.

# Appendix A: Evaluation of $H_{BA}$ as a Surface Integral

A simplified method for evaluating  $H_{\rm BA}$  is presented here, based on a method introduced by Bardeen.<sup>60</sup> The method is applicable

to all geometries of nonoverlapping wells. In the present model,  $H_{BA}$ , the main contribution to the thermal matrix element for electron transfer may be written as a volume integral over well B. That is

energy operator. (We write E rather than  $E_{\rm B}$ , since we consider

$$H_{\rm BA} = -V_0^{\rm B} \int_{\rm well B} \Psi_{\rm A} \Psi_{\rm B}^* d\tau \tag{A1}$$

where  $d\tau$  signifies a three-dimensional integral. In well B,  $-V_0^B\Psi_B^*$  equals  $(E-T)\Psi_B^*$  where T is the one-electron kinetic

<sup>(58)</sup> Halpern, J.; Orgel, L. E. Discuss. Faraday Soc. 1960, 29, 32-41. McConnell, H. M. J. Chem. Phys. 1961, 35, 508-515. (59) Beratan, D. N.; Hopfield, J. J. Am. Chem. Soc. 1984, 106,

<sup>(60)</sup> Bardeen, J. Phys. Rev. Lett. 1961, 6, 57-59.

 $E_A = E_B$ , as noted in the text. The method described in this Appendix is inapplicable unless the orbital energies  $E_A$  and  $E_B$  are equal.) Then eq A1 becomes

$$H_{\rm BA} = \int_{\rm well \, B} \Psi_{\rm A}(E - T) \Psi_{\rm B}^* \, \mathrm{d}\tau \tag{A2}$$

Since

$$\Psi_{\rm B}^*(E-T)\Psi_{\rm A}=0$$
 (A3) anywhere outside well A, the left-hand side of eq A3 can be

integrated over well B and subtracted from the integral of eq A2 without changing the value of  $H_{BA}$ . We thus obtain

$$H_{\rm BA} = -\int_{\rm well \, B} (\Psi_{\rm B}^* T \Psi_{\rm A} - \Psi_{\rm A} T \Psi_{\rm B}^*) \, d\tau \tag{A4}$$
 The latter can be rewritten as

... C 5.(3)

$$H_{\rm BA} = -\int_{\rm well\,B} \nabla \cdot (\Psi_{\rm B}^* \nabla \Psi_{\rm A} - \Psi_{\rm A} \nabla \Psi_{\rm B}^*) \, d\tau \qquad (A5)$$

Application of the divergence theorem<sup>61</sup> transforms this volume integral to a surface integral which may be evaluated on any surface that does not enclose well A. For analytical results, the choice of a plane between the centers of the wells proved particularly convenient.<sup>27</sup> For numerical calculations, we have found

it convenient to choose the surface as the boundary of well B. With this choice, 
$$H_{BA}$$
 becomes
$$H_{BA} = -\int_{S} \mathbf{n} \cdot (\Psi_{B} * \nabla \Psi_{A} - \Psi_{A} \nabla \Psi_{B} *) dS \qquad (A6)$$

where n is a unit vector normal to the surface of well B and dS is an area element of the surface S of well B. Thus, the only part

of 
$$(\Psi_B^*\nabla\Psi_A - \Psi_A\nabla\Psi_B^*)$$
 which needs to be calculated is the derivative normal to the surface, i.e. 
$$\mathbf{n}\cdot(\Psi_B^*\nabla\Psi_A - \Psi_A\nabla\Psi_B^*) = \Psi_B^*(\partial\Psi_A/\partial\xi_B) - \Psi_A(\partial\Psi_B^*/\partial\xi_B)$$

In eq A7,  $\xi_B$  denotes the coordinate  $\xi$  of the oblate-spheroidal coordinate system  $(\xi, \eta, \varphi)$  which has its origin at the center of well B. The normal derivative  $\partial \Psi_B^*/\partial \xi_B$  can be calculated directly

from the derivative with respect to  $\xi$  of individual oblate-spheroidal radial functions<sup>36</sup>  $R_{mn}(\xi)$ , centered at well B. ( $\Psi_B^*$  is an  $\eta$ -dependent sum of such functions). A three-point central difference approximation was used to calculate the derivative  $\partial \Psi_A/\partial \xi_B$ . In the several cases tested, it was found that at least three-place agreement was obtained with the three-dimensional integration for  $H_{BA}$  using a  $\Delta \xi = 0.001$ . The computation time for the two-dimensional integral (eq A6) was a factor of 6–10 times less

# Appendix B: Treatment of Multiconfiguration Excited States We assume here that in electron transfers involving porphyrin

than that for the three-dimensional one.

excited states the first excited singlet state is adequately described by the four-orbital model.<sup>39</sup> For concreteness the x-polarized transitions are considered. In representing the present wave functions, we omit all doubly occupied molecular orbitals; they are assumed to be unaffected by the presence or absence of the transferable electron. Furthermore, the  $\xi$ - and  $\eta$ -dependent parts of the wave functions need not be considered explicitly. The

two-electron singlet wave functions corresponding to primitive single excitations, for transitions polarized in the x direction, are

$$\psi_1 = \mathcal{A}[\cos 4\varphi_A(1) \cos 5\varphi_A(2)]\Phi$$

$$\psi_2 = \mathcal{A}[\sin 4\varphi_A(1) \sin 5\varphi_A(2)]\Phi$$
(B1)

$$\Phi = (\alpha(1)\beta(2) - \beta(1)\alpha(2))/2^{1/2}$$
 The number in parentheses denotes the electron in the given

orbital. The symbol  $\mathcal{A}$  is the antisymmetrizer operator which guarantees that the wave functions are antisymmetric under particle interchange. The effects of electron-electron interactions can be included by allowing for configuration interaction. Within

the four-orbital model<sup>39</sup> it is assumed that only the above two primitive excitations contribute significantly to the lowest excited singlet state. The secular equation which then determines the multiconfiguration excited state is

 $\begin{bmatrix} E_1 & H_{12} \\ H_{21} & E_2 \end{bmatrix} \begin{bmatrix} C_1 \\ C_2 \end{bmatrix} = E \begin{bmatrix} C_1 \\ C_2 \end{bmatrix}$  (B2)  $E_1$  and  $E_2$  are the energies of the primitive excitation functions in eq B1, and  $H_{12}$  (= $H_{21}$ ) is a two-electron interaction term. The

solutions of eq B2 are linear combinations of  $\psi_1$  and  $\psi_2$  which are then taken to model the states observed in the x-polarized Q and B bands of the porphyin. In the present model  $E_1 = E_2$  so the states obtained lead to  $C_1 = \pm C_2$ . However, upon examination of the asymmetric systems the spectra indicate that  $E_1 \neq E_2$  in general.<sup>38</sup> The mixing coefficients could be taken from semi-

to model the electronic wave functions. In what follows it is assumed for simplicity that  $C_1 = -C_2$ , but this assumption is not essential.

The thermal matrix element  $H_{\rm BA}$  is

empirical<sup>38</sup> or ab initio<sup>44</sup> calculations while still using  $\psi_1$  and  $\psi_2$ 

 $H_{\rm BA} = \langle \Psi_{\rm donor} | V_{\rm acceptor} | \Psi_{\rm acceptor} \rangle$ 

It is assumed that 
$$\Psi_{\text{donor}}$$
 the wave function before electron transfer,

corresponding to the first excited singlet state, is  $\Psi_{\text{donor}} = \frac{\mathcal{A}}{21/2}(\cos 4\varphi_{\text{A}}(1) \cos 5\varphi_{\text{A}}(2) - \sin 4\varphi_{\text{A}}(1) \sin 5\varphi_{\text{A}}(2))\Phi \text{ (B4)}$ 

Substituting in eq B3, 
$$H_{BA}$$
 becomes

.A

$$H_{\rm BA} = \frac{\mathcal{A}}{2^{1/2}} \langle (\cos 4\varphi_{\rm A}(1) \cos 5\varphi_{\rm A}(2) - \sin 4\varphi_{\rm A}(1) \sin 5\varphi_{\rm A}(2))\Phi | V_{\rm acceptor} | \Psi_{\rm acceptor} \rangle$$
 (B5)

Since the wave functions here are two-electron wave functions,  $V_{\rm acceptor}$  is of the form  $V_{\rm B}(1)+V_{\rm B}(2)$ . In choosing the wave function for the final state,  $\Psi_{\rm acceptor}$ , it is assumed that the electronic state on the acceptor can be represented by a single configuration, say  $\cos 5\varphi_{\rm B}$ . Similarly, the oxidized donor is represented by a

single-configuration state, either  $\cos 4\varphi_A$  or  $\sin 4\varphi_A$ . Then the possible  $\Psi_{\text{acceptor}}$  states are (again neglecting all doubly occupied orbitals)

$$\Psi_{\text{acceptor}} = \begin{cases} \mathcal{A}(\cos 4\varphi_{A}(1) \cos 5\varphi_{B}(2))\Phi \\ \mathcal{A}(\sin 4\varphi_{A}(1) \cos 5\varphi_{B}(2))\Phi \end{cases}$$
 (B6)

If one chooses  $\Psi_{\rm acceptor} = \mathcal{A}(\cos 4\varphi_{\rm A}(1)\cos 5\varphi_{\rm B}(2))\Phi$  and when  $(\sin 5\varphi_{\rm A}(2)|\cos 5\varphi_{\rm B}(2))=0$ , as is the case for all orientations in the present article,  $H_{\rm BA}$  becomes

$$H_{\rm BA} = \frac{1}{2^{1/2}} \langle \mathcal{A} \cos 4\varphi_{\rm A}(1) \cos 5\varphi_{\rm A}(2) \times |V_{\rm acceptor}| \mathcal{A} \cos 4\varphi_{\rm A}(1) \cos 5\varphi_{\rm B}(2) \rangle$$
 (B7)

In obtaining eq B7, we have performed the integrations over the spin variables. By expansion of eq B7, the dominant terms sum to yield (dropping the dummy indices)

$$H_{\mathrm{BA}} pprox rac{1}{2^{1/2}} \langle \cos 4\varphi_{\mathrm{A}} | \cos 4\varphi_{\mathrm{A}} \rangle \langle \cos 5\varphi_{\mathrm{A}} | V_{\mathrm{B}} | \cos 5\varphi_{\mathrm{B}} \rangle$$
 (B8)

The quantity in eq B8 is just  $1/2^{1/2}$  times the one-electron matrix elements given in the present paper. Therefore, the one-electron matrix elements given in the text are sufficient to discuss the orientation dependence of electron transfers involving such multiconfiguration states.

In eq B4-B8 the donor state is multiconfigurational and the

acceptor state is single-configurational (the former justified as in ref 38 and 39 and the latter justified as in ref 45 and 46). The reason why the  $|H_{\rm BA}|^2$  obtained from eq B8 differs by a factor of 2 from the single-configuration value used in the text is that in the former the donor wave function contains both cosine and sine components, one of which by symmetry does not contribute to  $H_{\rm BA}$  when the acceptor state is a single configuration.

<sup>(61)</sup> Reitz, J. R.; Milford, F. J. "Foundations of Electromagnetic Theory", 2nd ed.; Addison-Wesley: Reading, MA, 1967; p 13.